

Respirable dust characterization using SEM-EDX and FT-IR: A case study in an Appalachian coal mine

J. Gonzalez, N. Pokhrel, L. Jaramillo, C. Keles & E. Sarver

Department of Mining and Minerals Engineering, Virginia Tech, Blacksburg, USA

ABSTRACT: Respirable coal mine dust still represents a serious occupational hazard. Significant resurgence of lung disease among US coal miners in central Appalachia has highlighted the knowledge gap surrounding detailed dust characteristics. This paper presents a case study of dust characterization in a central Appalachian underground coal mine. Respirable dust samples were collected in the intake, near the feeder breaker, and downwind of an active roof bolter, as well as in three downwind locations during four separate continuous miner cuts. The dust was characterized using scanning electron microscopy with energy dispersive X-ray (SEM-EDX) to estimate particle size and mineralogy distributions, and Fourier Transform-Infrared (FT-IR) spectrometry to estimate silica and kaolinite content. SEM-EDX results were generally consistent with previous results in other mines, including indication of relatively high mineral content, especially aluminosilicates, but low coal content in dust samples collected near the roof bolter and continuous miner. The SEM-EDX and FT-IR results were in reasonable agreement for silica (quartz) mass content, which was below 10% in all samples based on the FT-IR. For kaolinite, which was typically around 20%, the SEM-EDX tended to overpredict the FT-IR – at most, measuring 37% kaolinite when the FT-IR measured 20%.

1 INTRODUCTION

Respirable dust exposures still represent a serious occupational hazard for many coal miners. In the US, the available dust monitoring data suggest that concentrations of respirable dust (Doney et al. 2019) and crystalline silica (i.e., dominated by quartz) (Agioutanti et al. 2019) in coal mines have generally been declining across all regions for the last few decades. Nevertheless, health surveillance data show a resurgence of occupational lung disease since the late 1990s (Blackley et al. 2016, 2018). The resurgence has been especially dramatic in the central Appalachian region (i.e., including eastern KY, southwestern VA, and much of WV), where the most severe and rapidly progressive forms of disease have been reported. Radiographic evidence indicates that crystalline silica exposures are a likely factor in such cases, and several studies including pathology have also shown significant burden of silicate (in addition to silica) particles in lung tissue (Cohen et al. 2016, Jelic et al. 2017).

Taken together, the above observations have prompted keen interest in the characteristics of respirable coal mine dust (NASEM 2018). It has been commonly speculated that the tendency to mine thinner and thinner coal seams in central Appalachia—and thus to mine more and more rock strata along with the coal—has gradually increased the mineral content in the respirable dust (Laney & Weissman 2014). Likewise, increased use and power of continuous mining equipment may have resulted in decreased particle sizes (Sapko et al. 2007). However, since routine dust monitoring in US mines only yields the respirable dust mass concentration (mg/m^3) and silica content (reported as % quartz), data on other metrics of interest is scarce.

Table 1. SEM-EDX mineralogy classes defined for respirable coal mine dust, and likely sources of particles (updated from Johann-Essex et al. 2017a).

Mineralogy Class	Abbreviation	Sources
Carbonaceous	C	Coal strata and diesel particulate matter
Mixed Carbonaceous	MC	Coal, roof/floor rock strata
Aluminosilicates - Kaolinite	AS-K	Roof/floor rock strata
Aluminosilicates - Other	AS-O	Roof/floor rock strata
Carbonates	CB	Rock dusting products
Heavy Minerals	HM	Metal sulfides/oxides in coal or rock strata, etc.
Other Silicates	OS	Roof/floor rock strata
Other	O	Other minerals, biological particles, etc.

To begin filling in the knowledge gap surrounding respirable dust characteristics, the authors' research group has been sampling and analyzing dust from US mines (e.g., see Sellaro et al. 2014, Johann Essex et al. 2017a, Sarver et al. 2019, Sarver et al. 2020). The use of scanning electron microscopy with energy dispersive X-ray (SEM-EDX) has been an important tool for that work. While not feasible for routine monitoring, it allows analysis of particle size and mineralogy distributions on filter samples. For practical comparison of dust constituents between different samples, defined mineralogy classes have been established that cover most particles found in coal mine dust (Table 1).

Heretofore, the particle-based SEM-EDX results have not been widely compared to other methods. One logical comparison is between SEM-EDX derived silica (S) and kaolinite (AS-K) contents and standard measures of quartz and kaolinite mass, such as achieved using Infrared (IR) spectroscopy. Indeed, the US National Institute for Occupational Safety and Health (NIOSH) has recently developed a direct on-filter Fourier Transform IR (FT-IR) method intended for analysis of quartz in respirable coal mine dust (Cauda et al. 2016); the method concurrently quantifies kaolinite since it must be used to correct the quartz result.

To gain further insights on respirable dust characteristics in central Appalachia, and offer preliminary comparisons between particle-based SEM-EDX and mass-based FT-IR results, this paper presents a case study from a coal mine in southern WV.

2 MATERIALS AND METHODS

2.1 Site details

The mine sampled for this study is a room and pillar operation in US MSHA District 12. It is extracting the Upper Alma coal seam, with an average thickness of 0.8 m. The average total mining height is about 2.4 m, including about 1.2 m of shale (roof), 0.2 m of sandy shale with quartz (floor), and 0.2 m of mudstone. The mine uses exhausting ventilation with line curtain at the face. The section sampled has seven entries; it operates two continuous miners (CM), two roof bolters, and four shuttle cars.

2.2 Dust sampling

Respirable dust sampling was conducted over two days in March 2020, in six key locations. The first three (intake, I; just downwind from an active roof bolter, B; adjacent to the feeder breaker, F) were sampled on Day 1. On Day 2, samples were collected at the other three locations (at the CM curtain mouth, CM1; at the next break downwind, CM2; and further downwind in the return, R; see Figure 1) during four separate but consecutive miner cuts. For Cuts 1 and 4, the cut depth was about 15 m and the scrubber was off. For Cuts 2 and 3, the cut depth was about 20 m and the scrubber was on.

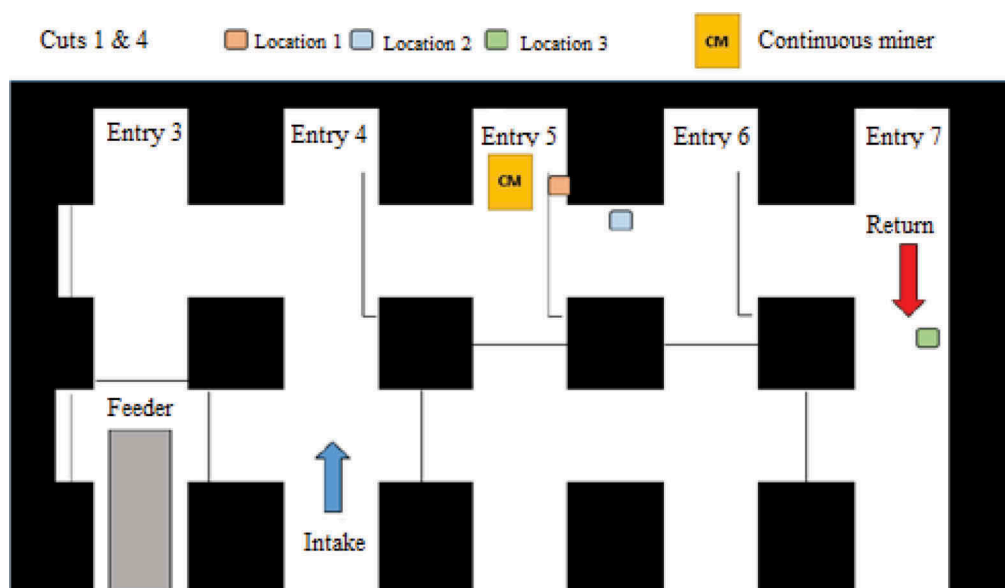


Figure 1. Schematic of sampling locations in the study mine for cuts 1 and 4. For cut 2, locations 1 and 2 were positioned at entry 7, and for cut 3 at entry 6.

In each location, samples were collected in sets as described below. In total, 15 sets were collected (i.e., I, B, F x 1, and CM1, CM2, R x 4). Each sample set contained four 37-mm filters: two track-etched polycarbonate (PC; 0.4 μ m pore size) appropriate for SEM-EDX, and two polyvinyl chloride (PVC; 5 μ m pore size) for gravimetric and FT-IR analysis. All filters were housed inside 2-piece styrene cassettes, and dust was sampled using Escort ELF pumps with 10-mm Dorr Oliver nylon cyclones (Zefon International, Ocala, FL) at 2.0L/min (i.e., d₅₀ of 3.5 μ m). For each sample set, the pumps were hung side by side using a metal frame, with the cyclone inlets oriented parallel to one another. Each sample set was collected over 1-3 hours, depending on the expected dust concentration or the time required for the miner cut.

2.3 Dust analysis

The PVC filters were pre-and post-weighed using a microbalance (Sartorius MSE6.6S, Göttingen, Germany) to allow gravimetric determination of respirable dust mass concentration in each location (i.e., using pump flow rate and sampling time).

The PVC filters were also used for direct-on-filter FT-IR analysis using an ALPHA II spectrometer (Bruker, Billerica, MA). For this, each filter was carefully removed from its cassette, placed into an FT-IR-compatible 4-piece cassette (Zefon International, Ocala, FL) and a 6-mm spot in the center of the filter was scanned using Bruker's OPUS software to produce the absorbance spectrum (4000 cm⁻¹ to 400 cm⁻¹ with a resolution of 4 cm⁻¹; 16 scans per sample). The spectrum was corrected for a blank PVC filter, then used to determine the mass (μ g) of quartz and kaolinite based on their characteristic peaks at 800 cm⁻¹ and 915 cm⁻¹, respectively. To convert measured peak areas to analyte mass, calibration models were used that were established by NIOSH (i.e., using pure quartz or kaolinite dust materials). A data correction based on Miller et al. (2013) was also applied to adjust for the fact that the study samples were collected in 2-piece cassettes, rather than 3-piece cassettes like NIOSH's calibration samples. Finally, the quartz (Q) and kaolinite (K) mass % on each sample could be computed using the total sample mass.

For the SEM-EDX analysis, 9-mm subsections were cut from one PC filter in each sample set, and sputter-coated with Au/Pd. The samples were analyzed with a FEI Quanta 600 FEG

Table 2. Classification criteria for each mineralogy class shown in Table 1 (updated from Johann-Essex et al. 2017b). Criteria are for supramicron particles examined using the SEM-EDX parameters stated in the text. Assumptions for short-to-intermediate dimension ratio (SI) and specific gravity (SG) are also shown.

Atomic %									Particle size to mass assumptions	
Class	O	Al	Si	C	Mg	Ca	Ti	Fe	SI	SG
C	<29	≤0.30	≤0.30	≥75	≤0.50	≤0.41	≤0.06	≤0.15	0.6	1.40
MC		<0.35	<0.35		≤0.50	≤0.50	≤0.60	≤0.60	0.6	1.40
AS-K ¹		≥0.35 (≥39)	≥0.35 (≥32)		(<15)	(<8)	(<13)	(<13)	0.4	2.60
AS-O ¹		≥0.35 (<39)	≥0.35 (<32)		(≥15)	(≥8)	(≥13)	(≥13)	0.4	2.60
OS ²			≥0.33						0.4	2.60
S ³			≥0.33						0.7	2.65
M		>1%					>1%	>1%	0.7	4.96
CB	>9				>0.5%	>0.5%			0.7	2.70

¹To differentiate AS-K from AS-O, additional limits for Al, Si, Mg, Ca, Ti and Fe are shown in parenthesis (normalized to exclude C and O)

²Additional limits for OS: $\text{Si}/(\text{Al}+\text{Si}+\text{Mg}+\text{Ca}+\text{Ti}+\text{Fe}) < 0.5$

³Additional limits for S: $\text{Al}/\text{Si} < 1/3$ and $\text{Si}/(\text{Al}+\text{Si}+\text{Mg}+\text{Ca}+\text{Ti}+\text{Fe}) \geq 0.5$

environmental SEM (FEI, Hillsboro, OR) equipped with a Bruker Quantax 400 EDX spectroscope (Bruker, Ewing, NJ). A computer-controlled routine described by Johann-Essex et al. (2017b) was used to select, size, and classify about 500 particles (1-10 μm) per sample; classification criteria are shown in Table 2. The routine was run using Bruker's Esprit software (Version 1.9), and the following SEM settings: 1,000x magnification, 12.5 mm working distance, 15 kV accelerating voltage, 5.5 μm spot size.

To convert SEM-EDX derived data on S and AS-K number % into estimates of S and AS-K mass %, assumptions for a short-to-intermediate dimension ratio (per class as shown in Table 2) were used to compute a volume for each particle; and an assumed specific gravity was used to translate particle volume to mass. Then, the total mass of S or AS-K particles in a sample was divided by the total mass of all particles (summed across all classes) to estimate the S and AS-K mass %, respectively. Finally, these values were compared with Q and K mass % values from the FT-IR analysis.

3 RESULTS AND DISCUSSION

Table 3 summarizes the results from all 15 sets of respirable mine dust samples. Relative dust concentrations (determined gravimetrically) are generally consistent with expectations based on specific sampling locations and the conditions in those locations. The dust concentration was very low in the intake, higher near the roof bolter, and was highest at the miner ventilation curtain mouth (CM1) – although there was wide variability in that location and no consistent trend with the application of the miner scrubber. Moving downwind from CM1, the dust concentration was reduced at CM2 and again at the R location. (It should be noted that the concentrations shown in Table 3 have not been converted to the BMRC MRE equivalency that is typically used for respirable dust monitoring in US coal mines, so these values should not be directly compared to MRE-corrected data.)

Mineralogy distributions determined by SEM-EDX are graphically displayed in Figure 2 and are generally consistent with results obtained in other central Appalachian mines (e.g., see Sarver et al. 2019, Sarver et al. 2020). Respirable dust in the intake air, while low in concentration, contains a variety of constituents, including those associated with the coal (C and MC particles) and rock strata (AS and S) and application of limestone rock dust (CB), which is

Table 3. Summary of results for all 15 sets of respirable mine dust samples. For gravimetric and FT-IR analysis, results are presented as an average of the two PVC samples analyzed in a given set. BD = below the limit of detection.

Location (miner cut, scrubber status)	SEM-EDX (number %)									FT-IR (mass %)		Grav. Conc. (mg/m3)
	C	MC	AS-K	AS-O	S	HM	CB	OS	O	Q	K	
I	35	18	6	15	10	1	12	2	2	BD	71	<0.1
F	8	15	9	54	4	2	4	0	3	6	13	1.5
B	0	1	27	68	3	0	0	0	1	9	22	0.5
Cut 1 CM1	2	9	19	64	3	0	1	0	1	4	19	4.5
OFF CM2	25	24	17	25	8	1	0	0	1	5	21	2.4
R	33	27	12	16	6	1	3	0	2	3	15	1.6
Cut 2 CM1	0	3	35	59	3	0	0	0	0	6	20	9.6
ON CM2	8	22	26	37	4	1	1	0	2	5	22	4.4
R	20	26	19	25	5	1	2	0	1	4	24	1.2
Cut 3 CM1	12	19	25	37	4	1	1	0	2	3	20	2.8
ON CM2	25	28	13	21	6	0	4	0	3	2	22	1.1
R	21	28	16	24	5	0	3	0	2	8	25	0.9
Cut 4 CM1	0	0	37	60	3	0	0	0	0	7	19	11.8
OFF CM2	1	1	30	67	1	0	0	0	0	7	20	7.5
R	30	24	17	21	5	1	1	0	1	3	20	3

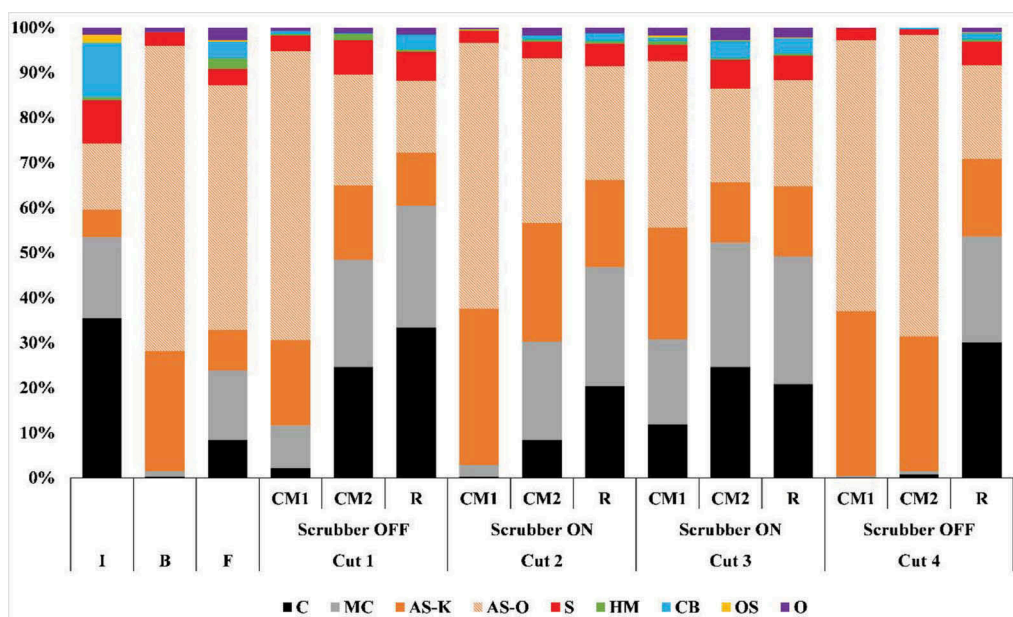


Figure 2. Mineralogy distribution (number %) of respirable dust particles in each sample set.

required in US mines to mitigate explosibility hazards. (It is noted that C particles can be associated with diesel particulates in some mines, but the study mine does not operate any diesel equipment and so C particles in this mine are considered most likely to be coal.) Near the roof bolter, nearly all of the dust appears to be sourced from the roof rock, whereas near the feeder, there is more coal content.

Just downwind from the continuous miner, the influence of rock-strata sourced dust appears very strong – with AS classes accounting for 62-97%, and AS+S accounting for 66-100%, of all classified dust particles in the CM1 location between the four different miner cuts. Coal-strata sourced dust (C+MC) accounted for most of the other dust in this location, up to 31%. SEM-EDX analysis of respirable dust in other mines, particularly thin-seam mines, has also yield inordinately high percentages of AS (or AS+S) particles dust near the mine face (Sarver et al. 2019, Johann-Essex et al. 2017a), although the cause for these observations has not been fully elucidated. One possibility is that very fine silicate dust being generated in the area is sticking to (or otherwise interfering with SEM-EDX analysis of) larger dust particles such as coal. In the current study, the highest AS (and AS+S) proportions in CM1 location samples were observed during Cuts 2 and 4, which also had the highest dust mass concentrations. Notably, no trend in mineralogy distribution could be discerned with the operation of the miner scrubber (i.e., OFF versus ON).

Moving downwind into the return airway, a consistent trend was observed wherein the proportion of AS+S decreased and that of C+MC increased. This may be due to additional sources of dust in the return, or reduced influence of very fine silicate particles on the SEM-EDX analysis of coal and other dust particles.

Figure 3 shows the overall particle size distribution by mineralogy class (top), sampling location (middle), and for the predominant classes (C, MC, AS, and S) in the CM1 and R locations downwind of the continuous miner (bottom). Across all six sampling locations, the variability in particle size can generally be summarized as C, MC \ll S \ll CB < AS (total). These are fairly consistent with observations in other mines using the same classification criteria (Sarver et al. 2020), which also showed that S particles are typically finer than other

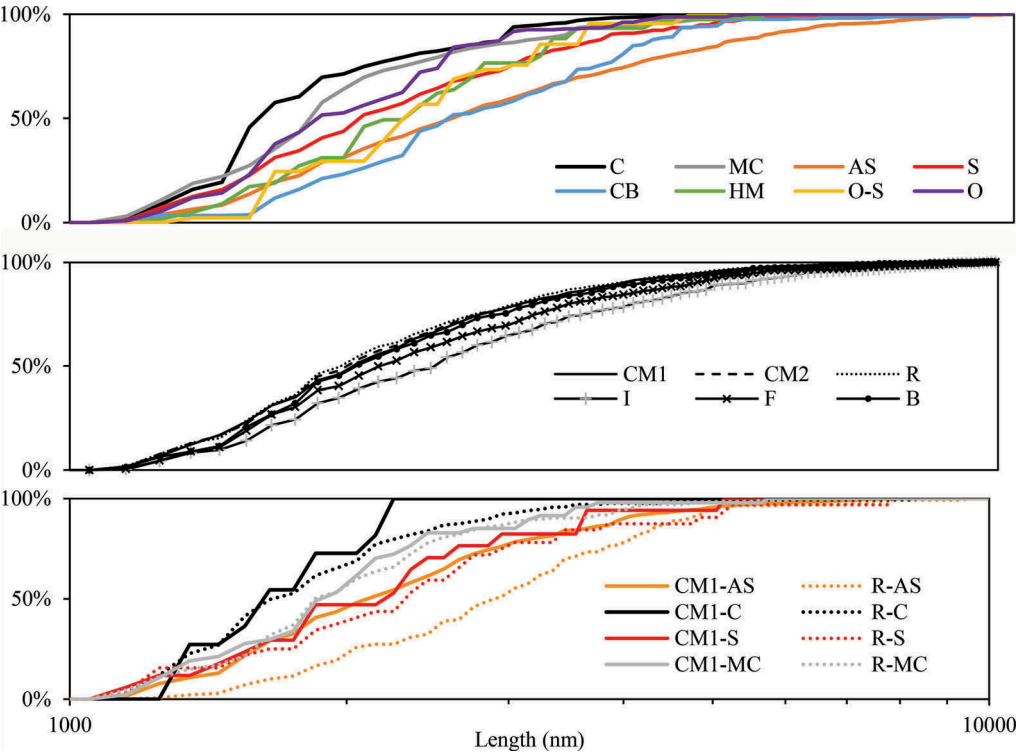


Figure 3. Cumulative size distributions of respirable dust particles by mineralogy class (top), sampling location (middle), and for the C, MC, AS (total), and S classes in the CM1 and R locations during miner Cut 1 (bottom). To construct the top plot, results were averaged across all six sampling locations; since four samples (one per cut) were analyzed in CM1 and R, results from each cut were first averaged to get a single dataset for each of these locations. For the middle plot, all particles in a given location were averaged.

predominant minerals (AS and CB), and that particles classified as C or MC are typically finer than all minerals. With respect to sampling location, variability in size can be summarized as CM1, CM2, R, B < F < I. Again, this is consistent with expectations; the finest particles occur nearest to active cutting and drilling.

To gain further insight on the dust moving downwind from the continuous miner, the bottom plot of Figure 3 shows particle size distributions for the CM1 and R locations during Cut 1, and results were similar for Cuts 2 and 4. (Note that only the C, MC, S, and AS classes are shown since these accounted for most particles.) Dust in each class is relatively fine at CM1 and becomes somewhat coarser by the time air moves into the return. The change in AS particle size distribution is most evident and is of particular interest since the very fine AS particles near the mine face could be influencing the SEM-EDX classification of other particles (due to interaction of AS and other particles, or interference of the fine AS with classification of other particles, see below). Notably, while the particles in each class are becoming coarser moving away from the dust source, the shift in mineralogy distribution illustrated in Figure 2 (from mostly AS to more C+MC) causes the overall size distribution of the dust in the CM1, CM2, and R locations to be quite similar.

Results from the SEM-EDX analysis were also compared to those from FT-IR, specifically to investigate how SEM-EDX derived S and AS-K content relate with FT-IR derived Q and K content, respectively. For this, the SEM-EDX data was used to estimate S and AS-K mass % values as described. Figure 4 shows the difference between the resulting SEM values and the FT-IR values for all sample sets in the study mine (with the exception of the intake sample set, for which the dust mass was too low to obtain FT-IR results). This comparison reveals reasonably good agreement for measurements of S/Q, in that the difference between the two methods (FT-IR Q% – SEM-EDX S%) was within $\pm 6\%$. However, given that all samples exhibited S/Q content (mass %) within a relatively tight range, further comparisons are needed to confirm that such agreement should be expected across a wider range of mass %. That said, the results presented here do seem to indicate that the S/Q agreement should hold over a wide range of total dust sample mass.

The comparison of SEM-EDX derived AS-K and FT-IR derived K in Figure 4 shows decent agreement. Based on the FT-IR results (Table 3), K was around 20% for most samples.

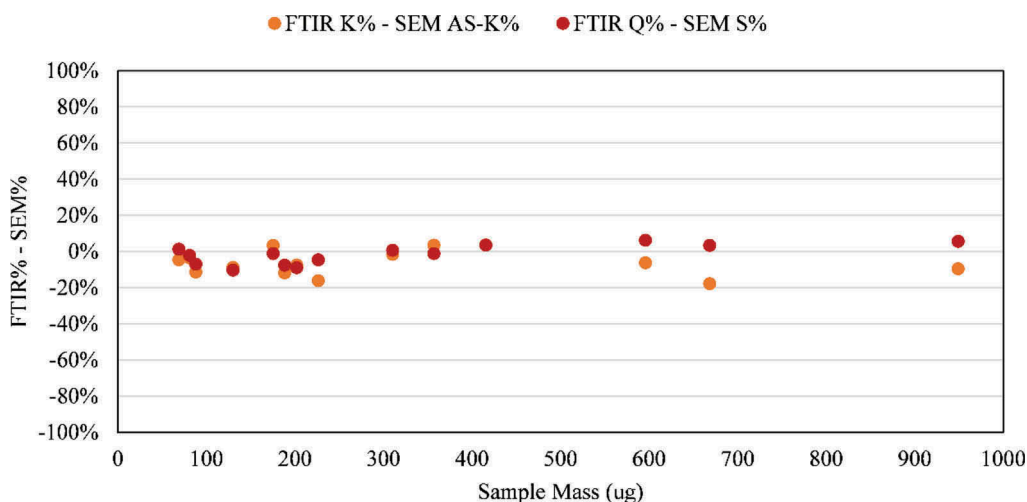


Figure 4. Comparison of FT-IR and SEM-EDX results for all sample sets, except that collected in the mine intake. The y-axis shows the difference between the FT-IR mass % for Q or K and the SEM-EDX mass % S or AS-K, respectively. For FT-IR measurements, the data represent the average of two PVC filters. Results are shown as a function of total dust mass (average measurement from the same two PVC filters).

The SEM-EDX tended to over-predict the FT-IR result; at most, it measured 37% AS-K when the FT-IR measured 20% K. There might be a number of factors contributing to these observations, including the possibility that the SEM-EDX misclassifies some AS particles as kaolinite that are in fact other alumino-silicates. Moreover, it is possible that coal or other particles, which are predominantly not alumino-silicate by mass, as classified as such based on sufficient Al and Si signals in their elemental spectra. As mentioned earlier, this could occur due to fine alumino-silicate particles sticking to the surface of other particles; it could also be due to ingrained impurities in particles. While care was taken to exclude agglomerates from the SEM-EDX analysis, the possibility that filter loading caused interference between particles in close proximity cannot be ruled out. Whatever the case, the findings presented here beg for further investigation of particle- versus mass-based measurements for respirable dust characterization.

4 CONCLUSIONS

Respirable dust exposures still represent an occupational health hazard for coal miners and a better understanding of dust constituents and particle sizes is needed. In this case study, dust characteristics determined by SEM-EDX were generally consistent with expectations based on similar analysis of samples collected in other central Appalachian mines. Unfortunately, no discernable trends could be observed in relation to the continuous miner's scrubber status – probably due to variability in geologic strata across the four miner cuts sampled. However, the ability to simultaneously sample at three locations downwind of the miner did provide new insights with respect to relative shifts in particle size and mineralogy distributions as dust is transported away from the mine face and diluted. Moreover, comparison of the SEM-EDX silica and kaolinite results with FT-IR quartz and kaolinite results yielded some important findings. The data for both analytes were in reasonable agreement, however, the SEM-EDX generally overpredicted the FT-IR for kaolinite. The reasons for this are not clear, but are likely related to the challenges of classifying individual particles in such complex samples.

ACKNOWLEDGEMENTS

The authors would like to thank The National Institute for Occupational Safety and Health for funding this work. We express heartfelt gratitude to the mine personnel that provided access to their operation and logistical assistance during the sampling campaign. The views and opinions expressed herein are solely those of the authors and do not imply any endorsement by research partners or funding source.

REFERENCES

- Agioutanti, E., Keles, C., Sarver, E. (2019). A thermogravimetric analysis application to determine coal, carbonate, and non-carbonate minerals mass fractions in respirable mine dust. *Journal of Occupational and Environmental Hygiene*. 17. 1–12.
- Blackley, D. J., Crum, J. B., Halldin, C. N., Storey, E., & Laney, A. S. (2016). Resurgence of Progressive Massive Fibrosis in Coal Miners — Eastern Kentucky, 2016. *MMWR. Morbidity and Mortality Weekly Report*, 65(49),1385–1389.
- Blackley, D.J., Reynolds, L.E., Short, C., Carson, R., Storey, E.S., Halldin, C.N., Laney, A.S. (2018). Progressive massive fibrosis in coal miners from 3 clinics in Virginia. *JAMA* 319 (5), 500–501.
- Cauda, E., Miller, A., & Drake, P. (2016) Promoting early exposure monitoring for respirable crystalline silica: Taking the laboratory to the mine site. *Journal of Occupational and Environmental Hygiene*. 13:3, D39–D45.
- Cohen, R. A., Petsonk, E. L., Rose, C., Young, B., Regier, M., Najmuddin, A., Abraham, J. L., Churg, A., & Green, F. H. Y. (2016). Lung pathology in U.S. coal workers with rapidly progressive

- pneumoconiosis implicates silica and silicates. *American Journal of Respiratory and Critical Care Medicine*, 193(6),673–680.
- Doney, B. C., Blackley, D., Hale, J. M., Halldin, C., Kurth, L., Syamlal, G., & Laney, A. S. (2019). Respirable coal mine dust in underground mines, United States, 1982-2017. *American Journal of Industrial Medicine*, 62(6),478–485.
- Jelic, T. M., Estalilla, O. C., Sawyer-Kaplan, P. R., Plata, M. J., Powers, J. T., Emmett, M., & Kuenstner, J. T. (2017). Coal mine dust desquamative chronic interstitial pneumonia: A precursor of dust-related diffuse fibrosis and of emphysema. *International Journal of Occupational and Environmental Medicine*, 8(3),153–165.
- Johann-Essex, V., Keles, C., & Sarver, E. (2017b). A computer-controlled SEM-EDX routine for characterizing respirable coal mine dust. *Minerals*, 7(1),14–16.
- Johann-Essex, V., Keles, C., Rezaee, M., Scaggs-Witte, M., & Sarver, E. (2017a). Respirable coal mine dust characteristics in samples collected in central and northern Appalachia. *International Journal of Coal Geology*, 182(September), 85–93.
- Laney, A.S., Weissman, D.N. (2014). Respiratory diseases caused by coal mine dust. *Journal of Occupational and Environmental Medicine*. 56 (010), S18–S22.
- Miller, A. L., Drake, P. L., Murphy, N. C., Cauda, E. G., LeBouf, R. F., & Markevicius, G. (2013). Deposition uniformity of coal dust on filters and its effect on the accuracy of FT-IR analyses for silica. *Aerosol Science and Technology*, 47(7), 724–733.
- National Academies of Sciences, Engineering, and Medicine (NASEM) (2018). Monitoring and Sampling Approaches to Assess Underground Coal Mine Dust Exposures. In *Monitoring and Sampling Approaches to Assess Underground Coal Mine Dust Exposures*.
- Sapko, M.J., Cashdollar, K.L., Green, G.M. (2007). Coal dust particle size survey of US mines. *J. Loss Prev. Process Ind.* 20 (4–6), 616–620.
- Sarver, E., Keles, C., & Rezaee, M. (2019). Beyond conventional metrics: Comprehensive characterization of respirable coal mine dust. *International Journal of Coal Geology*, 207(September 2018), 84–95.
- Sarver, E., Keles, C., Lowers, H., Zulfikar, R., Zell-Baran, L., . . . & Cohen, R. (2020). Mineralogic analysis of respirable dust from 24 underground coal mines in four geographic regions of the United States. In *2020 American Thoracic Society International Conference*. Virtual conference.
- Sellaro, R., Sarver, E. (2014). Characterization of respirable dust in an underground coal mine in Central Appalachia. *Trans. SME*, 336, 457–46.

PROCEEDINGS OF THE 18TH NORTH AMERICAN MINE VENTILATION SYMPOSIUM
(NAMVS 2021), JUNE 12-17, 2021, RAPID CITY, SOUTH DAKOTA, USA

Mine Ventilation

Editor

Purushotham Tukkaraja, Ph.D., QP

Mining Engineering & Management, South Dakota Mines, Rapid City, SD, USA



CRC Press

Taylor & Francis Group

Boca Raton London New York

CRC Press is an imprint of the
Taylor & Francis Group, an **informa** business

A BALKEMA BOOK

CRC Press/Balkema is an imprint of the Taylor & Francis Group, an informa business

© 2021 selection and editorial matter, Purushotham Tukkaraja, individual chapters, the contributors

“Auxiliary fan selection considering purchasing and energy costs based on fan curves”
authored by Enrique Acuna-Duhart and Michelle Levesque from Natural Resources Canada; and Juan Pablo Hurtado (non public servants). Copyright to Her Majesty the Queen in right of Canada as represented by the Minister of Natural Resources, 2021.

Typeset by Integra Software Services Pvt. Ltd., Pondicherry, India

The right of Purushotham Tukkaraja to be identified as the author of the editorial material, and of the authors for their individual chapters, has been asserted in accordance with sections 77 and 78 of the Copyright, Designs and Patents Act 1988.

All rights reserved. No part of this book may be reprinted or reproduced or utilised in any form or by any electronic, mechanical, or other means, now known or hereafter invented, including photocopying and recording, or in any information storage or retrieval system, without permission in writing from the publishers.

Although all care is taken to ensure integrity and the quality of this publication and the information herein, no responsibility is assumed by the publishers nor the author for any damage to the property or persons as a result of operation or use of this publication and/ or the information contained herein.

Library of Congress Cataloging-in-Publication Data

A catalog record has been requested for this book

Published by: CRC Press/Balkema

Schipholweg 107C, 2316 XC Leiden, The Netherlands

e-mail: enquiries@taylorandfrancis.com

www.routledge.com – www.taylorandfrancis.com

ISBN: 978-1-032-03679-3 (Hbk)

ISBN: 978-1-032-03681-6 (Pbk)

ISBN: 978-1-003-18847-6 (eBook)

DOI: 10.1201/9781003188476